



Fe₃O₄-SAHPG-Pd⁰ nanoparticles: A ligand-free and low Pd loading quasiheterogeneous catalyst active for mild Suzuki-Miyaura coupling and C—H activation of pyrimidine cores

Hamid Azizollahi¹ | Hossein Eshghi¹ | José-Antonio García-López²

¹Department of Chemistry, Faculty of Science, Ferdowsi University of Mashhad, Mashhad, 91775-1436, Iran

²Grupo de Química Organometálica, Universidad de Murcia, Campus de Espinardo, Murcia, 30100, Spain

Correspondence

Hossein Eshghi, Department of Chemistry, Faculty of Science, Ferdowsi University of Mashhad, Mashhad 91775-1436, Iran.
Email: heshghi@um.ac.ir

José-Antonio García-López, Grupo de Química Organometálica, Universidad de Murcia, Campus de Espinardo, Murcia 30100, Spain.
Email: joangalo@um.es

Funding information

Fundación Séneca Región de Murcia, Grant/Award Number: 19890/GERM/15; MICINN, Grant/Award Number: PGC2018-100719-B-I00; Research Council of Ferdowsi University of Mashhad, Grant/Award Number: 3/41215

This paper reports a green magnetic quasiheterogeneous efficient palladium catalyst in which Pd⁰ nanoparticles have been immobilized in self-assembled hyperbranched polyglycidole (SAHPG)-coated magnetic Fe₃O₄ nanoparticles (Fe₃O₄-SAHPG-Pd⁰). This catalyst has been used for effective ligandless Pd catalyzed Suzuki–Miyaura coupling reactions of different aryl halides with substituted boronic acids at room temperature and in aqueous media. Herein, SAHPG is used as support; it also acts as a reducing agent and stabilizer to promote the transformation of Pd^{II} to Pd⁰ nanoparticles. Also, this environmental friendly quasiheterogeneous catalyst is employed for the first time in the synthesis of new pyrimido[4,5-*b*]indoles via oxidative addition/C—H activation reactions on the pyrimidine rings, which were obtained with higher yield and faster than when Pd(OAc)₂ was used as the catalyst. Interestingly, the above-mentioned catalyst could be recovered in a facile manner from the reaction mixture by applying an external magnet device and recycled several times with no significant decrease in the catalytic activity.

KEY WORDS

cross-coupling reaction, hyperbranched polyglycidole, palladium nanoparticles, pyrimido[4,5-*b*]indoles, quasiheterogeneous catalyst

1 | INTRODUCTION

Cross-coupling reactions catalyzed by transition metals are one of the most efficient and direct strategies to form carbon–carbon bonds.^[1–4] Among various transition-metal catalysts, palladium nanoparticles (NPs) occupy a privileged position to achieve this goal.^[5] The key of the versatility and high activity of palladium NPs in cross-coupling reactions relies on the large surface-to-volume ratio of the NPs compared with the bulk phase, but such feature can also make them quickly aggregated to large particles in certain conditions.^[6–8] Therefore, they have

not sufficient stability during separation and recovery steps. To overcome this problem, immobilization of palladium particles on a heterogeneous and quasiheterogeneous support seems to be an efficient way, especially in the chemical industry.^[9] A broad range of supports such as polymers,^[10] silica,^[11] zeolites,^[12] carbon nanotubes,^[13,14] and graphene oxide^[15] have been explored so far to avoid these problems. Nowadays, hyperbranched polymers have attracted significant attention as catalyst support because of their ability to stabilize NPs.^[16–18] Among them, hyperbranched polyglycidole (HPG) has emerged as a great support due to

This paper is dedicated to Prof. Mehdi Bakavoli who passed away recently.

its characteristics: (i) it possess multiple anchoring sites, (ii) it acts as a reducing agent for metal ions to generate metal NPs via oxidation of the terminal hydroxyl groups and ether moieties,^[19–21] (iii) it has a stabilizer action due to dendritic structure, and (iv) can be easily prepared through a single step cationic ring-opening polymerization reaction,^[22] avoiding the harsh conditions generally required for the synthesis of dendrimers.^[23–25]

In particular, self-assembly of hyperbranched polymers gives them unique properties in comparison to those developed from linear polymers, for example, facile functionalization, morphology varieties, unusual mechanical properties, and excellent template ability.^[26,27] Through the self-assembly process, hyperbranched polymers form an organized structure via local van der Waals, Coulomb, or hydrophobic interaction and π - π stacking.^[28] Up to now, there is no report on the self-assembly of the HPG for catalytic applications and most of the reports focused on the modification and self-assembly of other hyperbranched polymers in order to diversify their functional groups^[20] and/or improve their solubility.^[16–18]

An interesting feature of heterogeneous catalyst relies on the possibility of their recovery and reutilization. Regarding this aspect, the introduction of magnetic NPs (MNPs) such as Fe_3O_4 has proven a useful strategy to make heterogeneous catalyst easily recoverable through the application of an external magnet.^[29–33] This strategy has been applied in the production of a range of heterogeneous transition-metal catalyst applied in cross-coupling reactions.^[8]

Herein, we report a straightforward approach to combine supporting property of self-assembled hyperbranched polyglycidole (SAHPG) for effective reduction and stabilization of palladium NPs in aqueous media, including the magnetic properties of Fe_3O_4 as

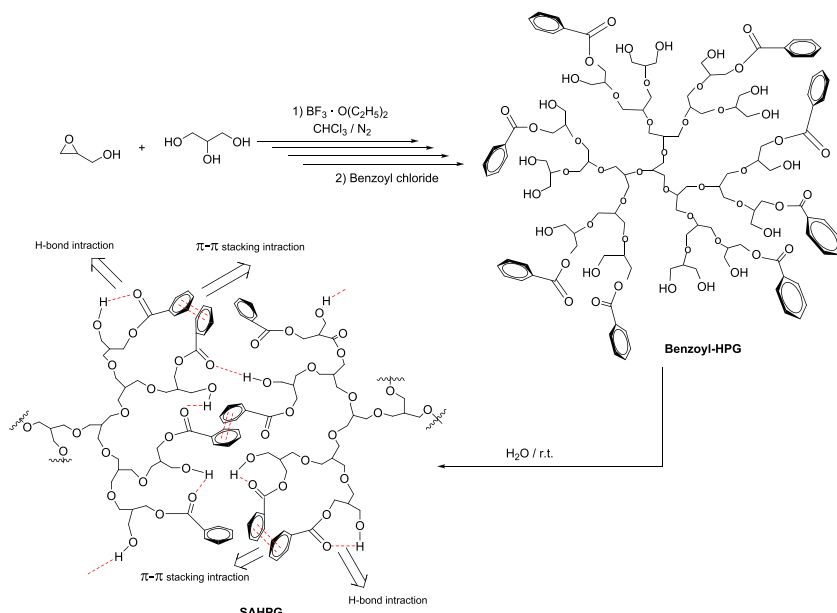
nontoxic and eco-friendly species to facilitate their separation and recycling (Fe_3O_4 -SAHPG-Pd⁰). Our interest in using SAHPG to synthesize a new palladium catalyst system is based on two phenomenal properties of HPG: (i) it can encapsulate the Pd NPs controlling their size and uniform distribution,^[34] and (ii) SAHPG can generate and stabilize Pd⁰ NPs arising from Pd²⁺ without the use of an external reducing agent through the coordination of free hydroxyl groups and ether moieties with the metal ions, while most polymers require a proper agent to reduce metal ions.^[18,19,21]

2 | RESULTS AND DISCUSSION

2.1 | Catalyst preparation

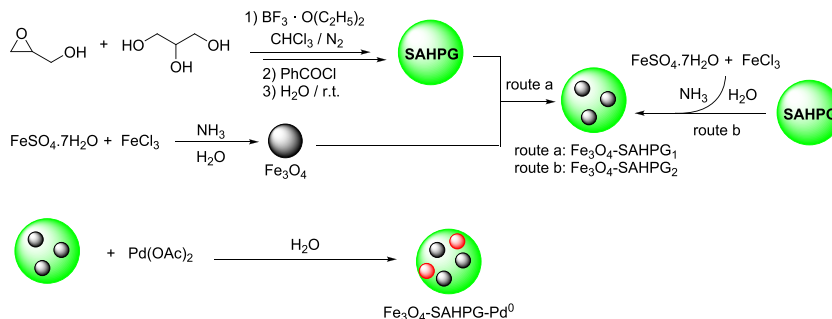
HPG with a variety of molecular weight were synthesized via cationic ring-opening multibranching polymerization reaction.^[19,20] In order to be benefitted from the unique characteristics of the self-assembled polymer, part of the terminal hydroxyl groups of HPG were reacted with benzoyl chloride to obtain benzoyl-HPG in first place, because the terminal hydrophilic OH groups in HPG do not allow to carry out a correct self-assembly process during the coating process of Fe_3O_4 in a polar solvent. The presence of aromatic groups in related polymeric materials is known to contribute to the self-assembly process through π - π interactions,^[35–39] improving also the stability of the micellar structure (Scheme 1).

There are two pathways for the synthesis of Fe_3O_4 -SAHPG, either separate synthesis of SAHPG and Fe_3O_4 , then dispersing Fe_3O_4 NPs on the SAHPG (route a, Fe_3O_4 -SAHPG₁, Scheme 2), or the synthesis Fe_3O_4 in situ



SCHEME 1 Synthetic route to self-assembled hyperbranched polyglycidole (SAHPG)

SCHEME 2 Schematic representation of Fe_3O_4 -SAHPG-Pd⁰



on the aqueous solution of SAHPG (route b, Fe_3O_4 -SAHPG₂, Scheme 2). In the reports published so far,^[18,21,40] functionalized Fe_3O_4 NPs have been used as a core and polymerization has been carried out in the surface of MNPs. Probably in such polymer support cases, immobilization of Fe_3O_4 cannot occur uniformly because the support is not able to prevent the aggregation of MNPs. However, *in situ* generation of Fe_3O_4 in an aqueous solution of SAHPG under stirring conditions enabled us to get Fe_3O_4 -SAHPG₂, where the magnetic Fe_3O_4 NPs are nicely dispersed into the polymeric material. Hence, this method avoided any undesired aggregation. Fe_3O_4 -SAHPG₂ was used as catalyst support to prepare the Fe_3O_4 -SAHPG-Pd⁰ by post-synthesis reaction of Pd(OAc)₂ with the support. Finally, the prepared catalyst was separated from the mixture by an external magnet and dried up in vacuum at 50°C for 6 h. The ICP-OES analysis of the catalyst showed a 16.8 weight% of Pd.

In many cases reported so far,^[41–44] after coating Fe_3O_4 particles with various polymers, they need to be modified with different groups to improve the solubility of the catalyst in a polar solvent (e.g., water, ethanol, and dimethylformamide); however, SAHPG on the Fe_3O_4 -SAHPG₂-Pd⁰ does not need any further modification to have a good solubility in these solvents. In contrast to the difficulties in separation and recovery of homogeneous catalysts,^[7,11,13,45] the Fe_3O_4 -SAHPG₂-Pd⁰ catalyst can be separated easily by an external magnetic field and recycled several times with no noticeable loss in the activity (see below). The new catalyst was characterized by various techniques, such as Fourier-transform infrared (FT-IR), scanning electron microscopy (SEM), transmission electron microscopy (TEM), dynamic light scattering (DLS), vibrating sample magnetometer (VSM), thermogravimetric analysis (TGA), X-ray diffraction (XRD), and X-ray photoelectron spectroscopy (XPS).

To confirm the synthesis of the catalyst, FT-IR spectra of (a) Fe_3O_4 , (b) HPG, (c) self-assembled HPG (SAHPG), (d) Fe_3O_4 -SAHPG₂, and (e) Fe_3O_4 -SAHPG₂-Pd⁰ were carried out (Figure 1). As shown in Figure 1a, the FT-IR spectrum of Fe_3O_4 MNPs shows a broad band at 578 cm⁻¹ corresponding to the stretching of the Fe—O

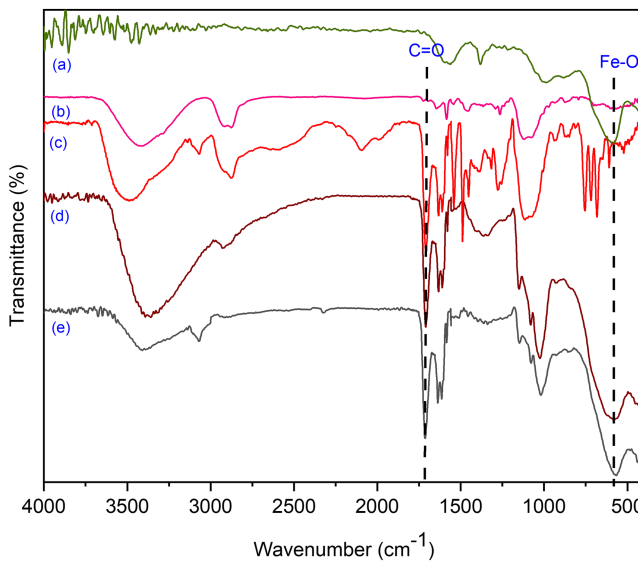


FIGURE 1 Fourier-transform infrared (FT-IR) spectra of (a) Fe_3O_4 , (b) hyperbranched polyglycidole (HPG), (c) self-assembled hyperbranched polyglycidole (SAHPG), (d) Fe_3O_4 -SAHPG, and (e) Fe_3O_4 -SAHPG₂-Pd⁰

bond. In the spectrum of the HPG, Figure 1b, the broad band at 3377 cm⁻¹ was attributed to a hydroxyl group.

To further verify the structural features including size distribution and surface morphology of Fe_3O_4 -SAHPG₂-Pd⁰ NPs, TEM and particle size histogram (DLS) were used (Figure 2). As can be seen in Figure 2a, the synthesized Fe_3O_4 -SAHPG₂-Pd⁰ revealed rounded magnetic nanoparticles distributed uniformly into the polymeric structure as a composite material which is probably arising from the great template ability of SAHPG. The Fe_3O_4 MNPs are characterized by a diameter of 20 nm as confirmed by TEM analysis (Figure 2b). We observed that when the route a (Scheme 2) was followed for the synthesis of Fe_3O_4 -SAHPG₁, as can be seen in (Figure 2c,d), the Fe_3O_4 NPs were aggregated, which was probably due to the low dispersity of MNPs into the SAHPG polymer structure. While in the route b a very good dispersion of magnetite NPs in the HPG and a nearly uniform distribution of particle size was observed (Figure 2a). So the *in situ* method (Scheme 2, route b) was selected as the main

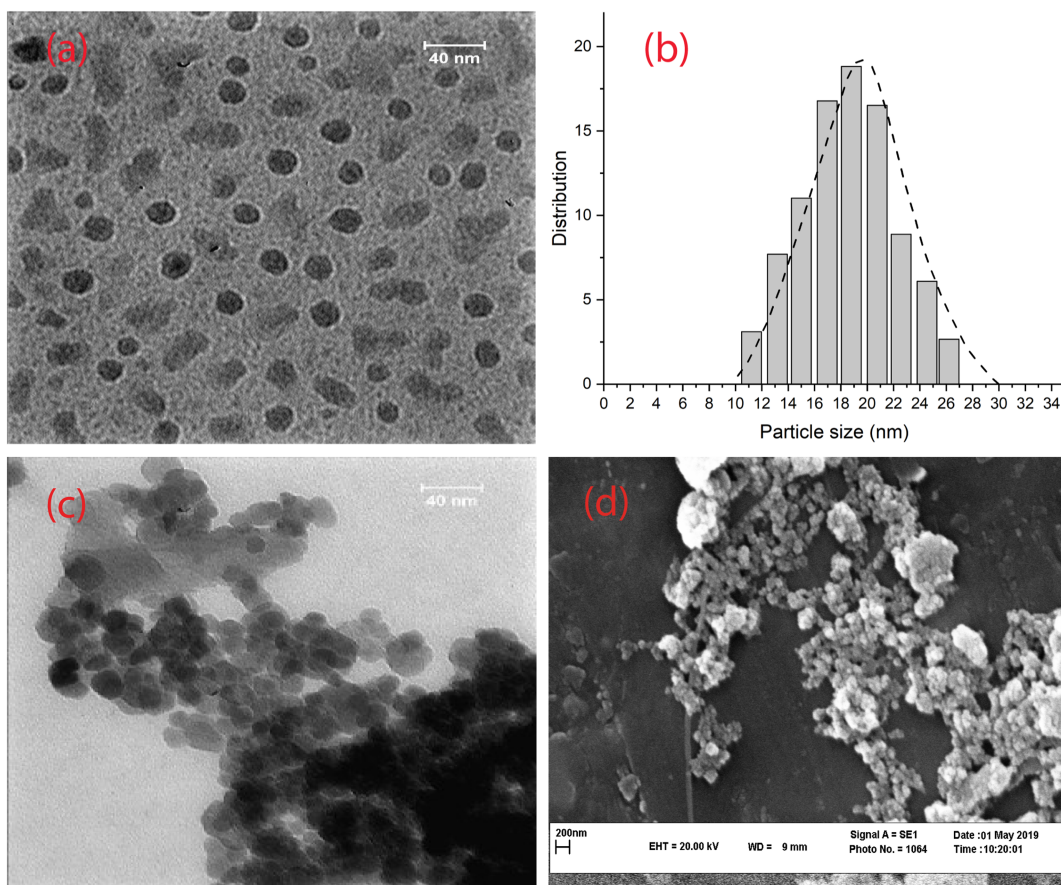


FIGURE 2 Transmission electron microscopy (TEM) image of (a) Fe_3O_4 -SAHPG₂-Pd⁰, (b) particle size histogram of Fe_3O_4 NPs, (c) TEM image of Fe_3O_4 -SAHPG₁, and (d) scanning electron microscopy (SEM) image of Fe_3O_4 -SAHPG₁

procedure for the synthesis of final catalyst Fe_3O_4 -SAHPG₂.

To investigate magnetic properties of Fe_3O_4 and Fe_3O_4 -SAHPG₂-Pd⁰ NPs, vibrating sample magnetometer (VSM) was used. As illustrated in Figure 3, superparamagnetic behavior was confirmed for the obtained NPs which were seized from the Fe_3O_4 core. The magnetization saturation (MS) value of Fe_3O_4 and Fe_3O_4 -SAHPG₂-Pd⁰ NPs was equal to 57 and 39 emu g⁻¹, respectively. Comparing with Fe_3O_4 MNPs, the MS value of Fe_3O_4 -SAHPG-Pd⁰ NPs was lower, which occurred upon dispersion of Fe_3O_4 MNPs in the SAHPG support. However, the magnetic property was high enough to recycle from the crude by the application of an external magnetic field.

In order to get more information on the crystallographic structure, chemical composition, and physical properties of Fe_3O_4 , Fe_3O_4 -SAHPG, and Fe_3O_4 -SAHPG₂-Pd⁰, XRD technique was used (Figure 4). As shown in Figure 4a, the Fe_3O_4 NPs were characterized by the diffraction peaks located approximately at $2\theta = 30.2^\circ$ (220), 35.6° (311), 43.1° (400), 53.2° (422), 57.1° (511), and 62.8° (440) which can be attributed to the cubic structure of

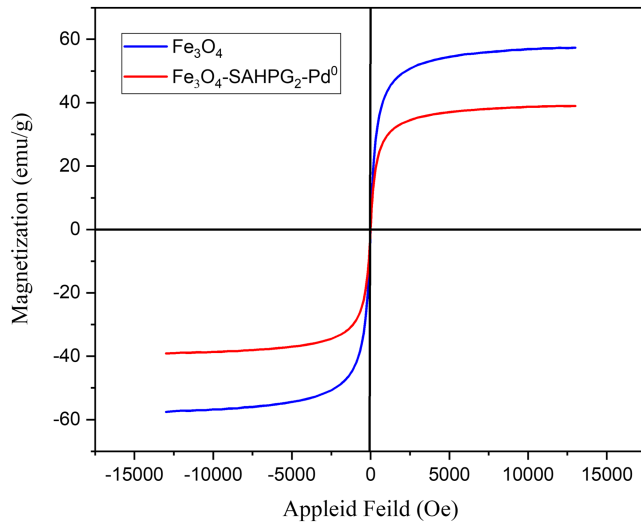


FIGURE 3 Magnetization hysteresis loops at room temperature (vibrating sample magnetometer [VSM])

Fe_3O_4 MNPs.^[5] In Figure 4c, after grafting the Fe_3O_4 -SAHPG with Pd NPs, the appearance of three new peaks at $2\theta = 40.1^\circ$ (111), 46.5° (200), and 68.0° (220) are imputed to the face-centered cubic system Pd⁰. The

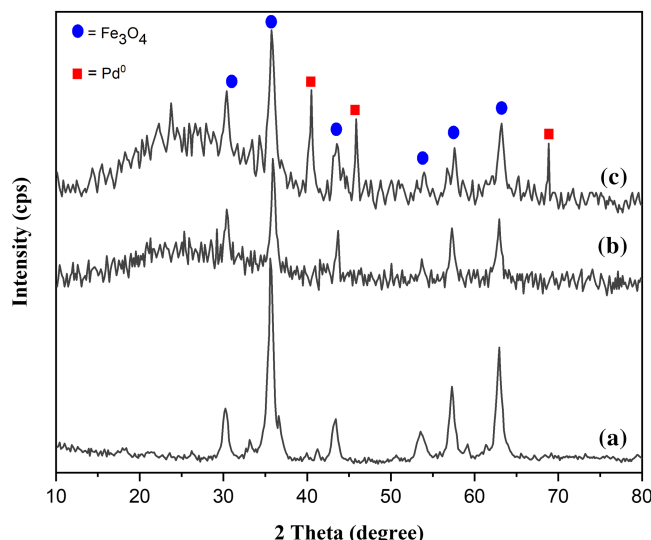


FIGURE 4 X-ray diffraction (XRD) patterns of (a) Fe_3O_4 , (b) $\text{Fe}_3\text{O}_4\text{-SAHPG}_2$, and (c) $\text{Fe}_3\text{O}_4\text{-SAHPG}_2\text{-Pd}^0$

observation of additional crystalline phase of Fe_3O_4 and $\text{Fe}_3\text{O}_4\text{-HPG}$ in the XRD pattern of $\text{Fe}_3\text{O}_4\text{-SAHPG}_2\text{-Pd}^0$ is a proof for embedding Fe_3O_4 NPs in the SAHPG. The chemical modification makes the peaks intensity decrease.

To investigate the coordination state of the embedded palladium enclosed by Fe_3O_4 -SAHPG, XPS analysis was accomplished. As can be seen in Figure 5, two bands centered at the binding energies 335.3 and 340.7 eV are attributed to Pd^0 ($3\text{d}_{5/2}$ and $3\text{d}_{3/2}$, respectively), which indicate that the Pd NPs are present in the nanocomposite structure of $\text{Fe}_3\text{O}_4\text{-SAHPG}_2\text{-Pd}$ as metallic state. The difference between observed and standard binding energy of Pd^0 is due to the higher density around the palladium species on the catalyst. The fitted peaks at

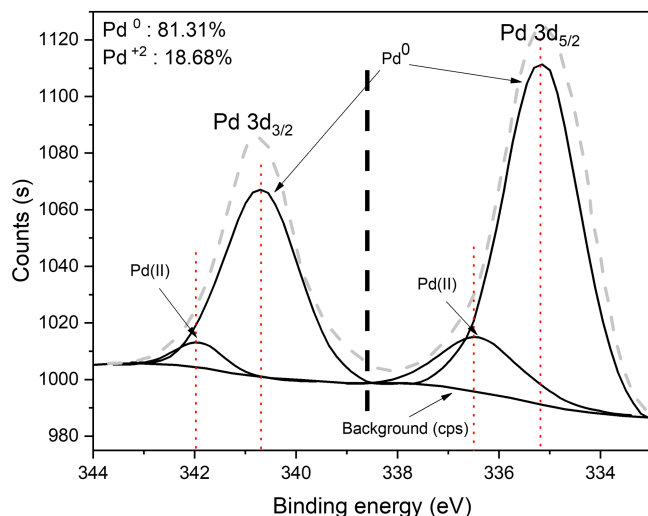


FIGURE 5 X-ray photoelectron spectroscopy (XPS) analysis

336.4 and 341.9 eV corresponded to the oxidized Pd^{2+} ($3\text{d}_{5/2}$ and $3\text{d}_{3/2}$, respectively) which are in agreement with the values reported in the literature.^[23–25] Measuring out the area under the peaks shows that the percentage of the Pd^0 and Pd^{2+} are 81.31 and 18.68, respectively (Figure 5).

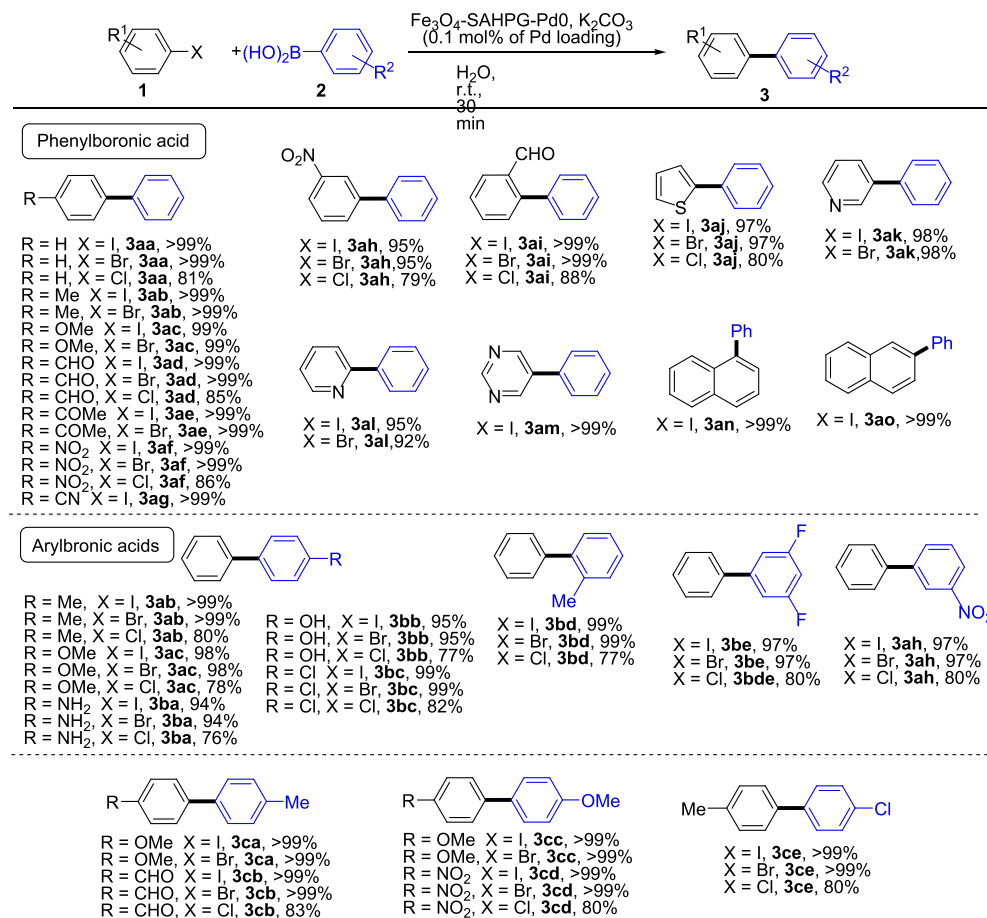
To prove the efficiency of the $\text{Fe}_3\text{O}_4\text{-SAHPG}_2\text{-Pd}^0$ nanocatalyst, the coupling of iodobenzene with phenylboronic acid was selected as a standard model reaction for Suzuki–Miyaura cross-coupling. An initial reaction of **1a** with **2a** in the presence of our catalyst (1 mol% of Pd regarding the substrate) and 1.5 equiv. of K_2CO_3 in H_2O at room temperature gave almost full conversion of the starting materials, affording the biaryl product **3a**.

In order to optimize the reaction conditions, we tested several parameters affecting the result of the reaction, such as temperature, base, and catalyst loading (see Table S1). Because $\text{Fe}_3\text{O}_4\text{-SAHPG}_2\text{-Pd}^0$ nanocatalyst has good solubility in water and also it is stable under aerobic conditions, we focused our initial investigation on the effect of various types of base, temperature, and palladium amount on the standard model reaction in aqueous media and the presence of air. The results of the model reaction indicated that the use of K_2CO_3 as a base and an amount of $\text{Fe}_3\text{O}_4\text{-SAHPG}_2\text{-Pd}^0$ equivalent to 0.1 mol% of Pd NPs provided the coupling product in more than 99% yield at room temperature after 30 min. No significant difference was observed in the yield of the reaction when the temperature was risen up to 80°C. Using other bases such as Et_3N and NaOAc led to lower yield of **3a**, so K_2CO_3 was selected as the base. Next, we tested the amount of catalyst and observed that lower loading of $\text{Fe}_3\text{O}_4\text{-SAHPG}_2\text{-Pd}^0$ were not effective. Upon establishing the optimized conditions to obtain biaryl products, we proceeded to study the scope of the reaction. We found that aryl iodides and bromides **1** bearing both electron-donating/electron-withdrawing groups gave excellent yields of biaryls **3** (Scheme 3). Also, we were interested in investigating the behavior of $\text{Fe}_3\text{O}_4\text{-SAHPG}_2\text{-Pd}^0$ in the Suzuki–Miyaura cross-coupling reaction of substituted aryl chlorides and arylboronic acids.

We observed a reasonable yield for the cross-coupling process at room temperature (Scheme 3) for aryl chlorides, although the reaction required slightly longer time than aryl iodides and aryl bromides, in comparison with reported works.^[46,47]

The catalyst could be easily removed from the reaction mixture and reused with no significant loss of activity for seven cycles (Tables 1 and S2).

In order to determine the catalytically active species in the Suzuki cross-coupling reaction, we performed a poisoning test. After 8 min of starting the reaction of



S C H E M E 3 Scope of the Suzuki–Miyaura cross-coupling

T A B L E 1 Recycling of Pd catalyst in the Suzuki–Miyaura cross-coupling reaction under the optimized reaction conditions

Entry	Cycle	Time (min)	Isolated yield (%)	TON ^a	TOF (h ⁻¹) ^b
1	1st	30	>99	>999.9	>1999.8
2	2nd	30	>99	>999.9	>1999.8
3	3rd	30	>99	>999.9	>1999.8
4 ^c	4th	30/35	98/>99	980/>999.9	1960/>1714.8
5 ^c	5th	30/40	98/>99	980/>999.9	1960/>1499.8
6 ^c	6th	30/45	95/>99	950/>999.9	1900/>1333.2
7 ^c	7th	30/60	92/>99	920/>999.9	1840/>999.9

Note: Reaction conditions: Fe₃O₄-SAHPG₂-Pd⁰ (0.1 mol% Pd), iodobenzene (1 mmol), phenylboronic acid (1.1 mmol), 1.5 equiv. base, 3-ml solvent.

^aTON = mmol of products/mmol of catalyst.

^bTOF = TON/time.

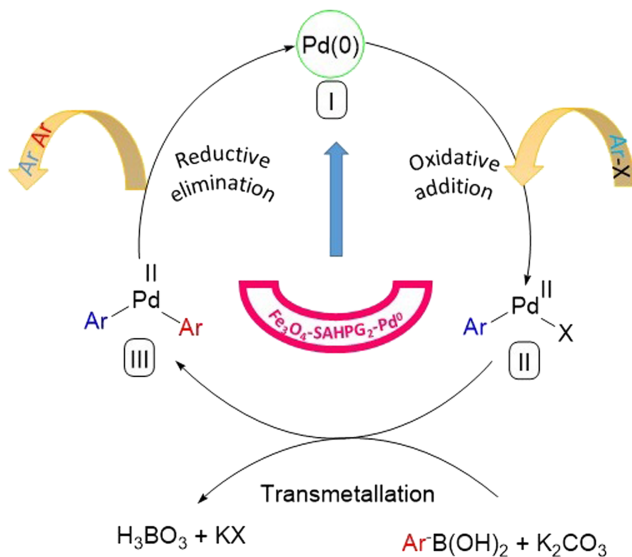
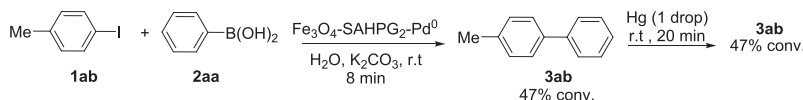
^cIn the second columns, second numbers are related to isolated yield after 35, 40, 45, and 60 min.

1-iodo-4-methylbenzene **1ab** and phenylboronic acid **2aa** (Scheme 4), one drop of mercury was added to the crude. We observed that the reaction completely halted (see Figures S9 and S10) These results show most likely palladium(0) species arising from palladium acetate are the catalytically active species in this reaction.

The mechanism of Suzuki–Miyaura coupling is shown in the Scheme 5. The first step is the oxidative addition of the aryl halide to Pd(0), arising from the

Fe₃O₄-SAHPG-Pd⁰, generating the organometallic intermediate II. Next, transmetalation of intermediate II with aryl boronic acid in the presence of K₂CO₃ can lead to the intermediate III. Finally, reductive elimination of biaryl compound restores the Pd(0), completing the catalytic cycle.

To indicate the efficiency of our catalyst, the catalytic activity of Fe₃O₄-SAHPG₂-Pd⁰ was compared with that of some previously reported for the Suzuki–Miyaura cross-

SCHEME 4 Mercury-amalgamation test**SCHEME 5** Mechanistic pathway for Suzuki–Miyaura cross-coupling

coupling of aryl halides with phenylboronic acid (Table 2). Although all of the listed catalysts can achieve the desired product in good to excellent yield, our catalyst can perform the Suzuki coupling under greener and milder reaction conditions. Compared with previously reported supported Pd catalyst employed for the Suzuki coupling reaction (Table 2), the use of hazardous solvents (Table 2, Entries 4–6), longer reaction time (Table 2,

Entries 1–6), or high temperatures (Table 2, Entries 1–8) are avoided. Furthermore, some of these methods may present disadvantages for the recovery and reusability of the catalyst (Table 2, Entry 8).

In order to determine the heterogeneity nature of the $\text{Fe}_3\text{O}_4\text{-SAHPG}_2\text{-Pd}^0$ catalyst system, the hot filtration test was performed. The reaction of 1-iodo-4-methylbenzene with phenylboronic acid under the optimized reaction conditions was selected as a model reaction. After 10 min, the catalyst was separated by an external magnetic field (49% ^1H -NMR yield, Figures S11 and S12), and the reaction was allowed to continue without the catalyst for 1 h. The crude ^1H -NMR showed no further progress in the coupling reaction even after an extended time, which indicated that no significant leaching of palladium NPs took place during the catalytic reaction (see Figures S11 and S12). This result demonstrated the heterogeneous nature of our catalyst. The ICP-OES analysis of the filtrate showed that there is no leaching of the palladium after 10 min. In the course of our investigations devoted to the synthesis of new heterocyclic compounds with interesting pharmacological properties, we were interested in the examination of the ability of the $\text{Fe}_3\text{O}_4\text{-SAHPG}_2\text{-Pd}^0$ catalyst to accomplish oxidative addition/C–H activation reactions on *N*-(2-iodophenyl)-*N*-substituted pyrimidine-4-amine substrates, in order to achieve the synthesis of new derivatives of the 9-substituted-9*H*-pyrimido[4,5-*b*]indole core. There are various synthetic routes to prepare pyrimido[4,5-*b*]indole

TABLE 2 Comparison of various catalysts in the Suzuki–Miyaura cross-coupling of 4-halobenzenes with phenylboronic acid

Entry	Catalyst	x	Solvent	Base	Temp (°C)	Time (h)	Yield (%)	Ref.
1	MOP-Pd	I/Br/Cl	H_2O : EtOH	K_3PO_4	80	3	97/82/–	Wu et al. ^[48]
2	CNT– Fe_3O_4 –PTh–Cu (I)	I/Br/Cl	H_2O : EtOH	K_2CO_3	80	1/1.1/4	90/85/55	Akbarzadeh et al. ^[49]
3	MP-TPy/Pd	I/Br/Cl	H_2O : EtOH	K_2CO_3	80	2/4/10	98/95/92	Targhan et al. ^[50]
4	Pd@TMC-Bpy COF	I/Br/Cl	Ethyl lactate	K_2CO_3	90	–/1.5/–	–/95/–	Han et al. ^[51]
5	GO/NiTAPP	I/Br/Cl	Dioxane	K_3PO_4	80	1/1/2.5	95/92/60	Keyhaniyan et al. ^[52]
6	Pdn-p-2	I/Br/Cl	DMF	K_2CO_3	110	4/–/–	94/–/–	Dutta and Sarkar ^[53]
7	Pd- γ - Fe_2O_3	I/Br/Cl	H_2O	NaOH	80	–/0.5/–	–/95/–	Paul et al. ^[54]
8	$\text{NiCl}_2(\text{PPh}_3)_2/\text{PPh}_3$	I/Br/Cl	Toluene	K_3PO_4	100	–/–/2	–/–/87	Inada and Miyaura ^[55]
9	$\text{Fe}_3\text{O}_4\text{-SAHPG}_2\text{-Pd}^0$	I/Br/Cl	H_2O	K_2CO_3	r.t.	0.5/0.5/1	>99/ >99/85	Present work

rings reported in the literature, for instance, (a) ring closure of 2,3-functionalized indoles with CN moieties such as formamide or cyanamide^[56]; (b) reaction of benzylidenindolenine borate derivatives with amidines, thiourea, and guanidines^[57]; (c) azidouraciles cyclization^[58]; and (d) the reaction of glycine ethyl ester with 2,4,6-trichloropyrimidine. The downsides of these methods are low to medium yielding rates, volatile solvent usage, and the need of additional steps to get the desired products. Moreover, a palladium-catalyzed reaction in pyrimidine systems has been reported.^[59] It involved the intramolecular arylation of pyridine ring where oxidative addition occurs on the C5 position of pyrimidine, followed by C—H activation on the aryl ring, giving rise the pyrimido[4,5-*b*]indole scaffold. In spite of the availability of these synthetic methods, a general route which incorporates a different range of substitution patterns is highly desirable.

We tested an initial reaction of the compound **4a** in the presence of 10 mol% of Pd(OAc)₂, 20 mol% of PPh₃, and 1.5 equiv. of K₂CO₃ in toluene at 80°C to investigate the feasibility of this reaction. We observed that the intramolecular cyclization was complete after 8 h to afford the compound **5a** in 63% ¹H-NMR yield. The screening of the amount of Pd(OAc)₂/PPh₃ (Tables 3 and S3) indicated that 10 mol% of catalyst loading could perform the intramolecular coupling reaction in moderate yield and the efficiency did not change with higher loading amounts of catalyst. To evaluate the applicability of Fe₃O₄-SAHPG₂-Pd⁰ as a catalyst to synthesize pyrimido[4,5-*b*]indole rings, the same experiment was repeated with Fe₃O₄-SAHPG₂-Pd⁰ (1 mol% of Pd regarding the substrate) obtaining compound **5a** (91% ¹H-NMR yield) in milder conditions and shorter time in comparison with Pd(OAc)₂/PPh₃ as palladium source.

Likely in our catalyst, the oxidative addition of Pd in the carbon–halogen bond and/or C—H activation on the C5 of pyrimidine are much faster than in the case when Pd(OAc)₂ is used as the metal source. According to the ¹H-NMR of the crude mixture, Fe₃O₄-SAHPG₂-Pd⁰ can perform this reaction without any side reaction such as homocoupling, which occur in higher extension with Pd(OAc)₂.

Compounds **5i–5l** bearing different secondary amines can be synthesized through either the substitution reaction of various secondary amines on the C2 of pyrimidine followed by the oxidative addition/C—H activation reactions or initial oxidative addition/C—H activation and subsequent reaction with the secondary amines (Scheme 6). A plausible mechanism to explain the formation of compounds **5** is depicted in Scheme 7. The initial oxidative addition of compound **4** leads to intermediate **A**, which undergoes C—H activation reaction affording intermediate **B**. Next, a reductive elimination takes place in intermediate **B** leading to synthesis pyrimido[4,5-*b*]indolets and regeneration of active catalytic species Pd⁰ for the next run.

3 | EXPERIMENTAL

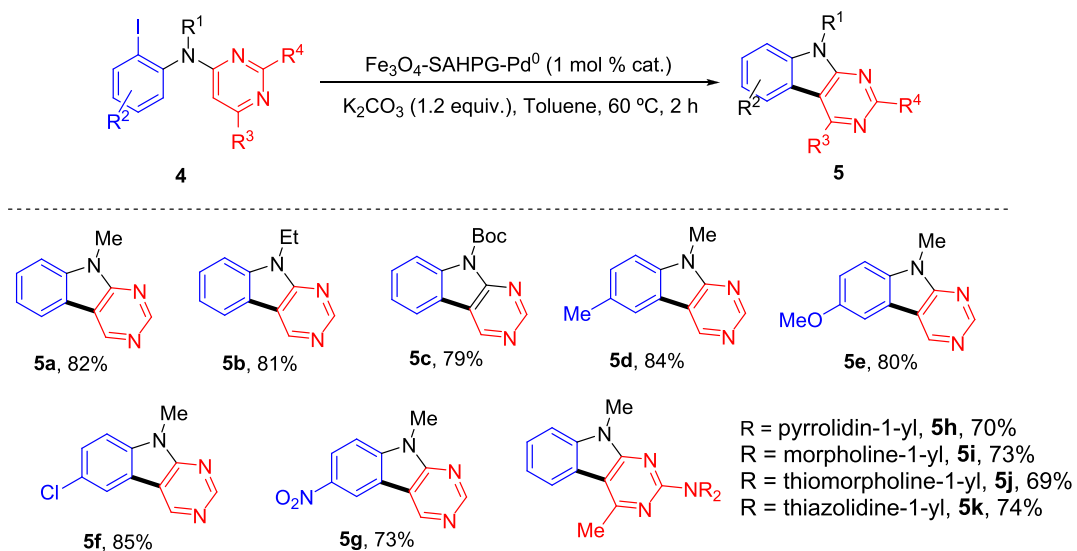
3.1 | Synthesis of Fe₃O₄-SAHPG-Pd⁰

Magnetic hyperbranched polyglycidole (Fe₃O₄-SAHPG) (0.5 g) was added to a suspension of Pd(OAc)₂ (0.5 g, 2.2 mmol) in water (40 ml). The mixture was stirred overnight at room temperature overnight. The resulting solid was isolated by separation from the reaction mixture with an external magnet device, washed with water, and then dried at room temperature to give Fe₃O₄-SAHPG-Pd⁰

TABLE 3 Optimization studies and screening the amount of the catalyst to synthesis pyrimido[4,5-*b*]indole

Entry	Catalyst system	Solvent	Catalyst amount (mol% Pd)	Yield (%)
1	Pd(OAc) ₂ /P(Ph) ₃	Toluene	2	20
2	Pd(OAc) ₂ /P(Ph) ₃	Toluene	5	45
3	Pd(OAc) ₂ /P(Ph) ₃	Toluene	10	63
4	Pd(OAc) ₂ /P(Ph) ₃	Toluene	20	65
5	Fe ₃ O ₄ -SAHPG ₂ -Pd ⁰	Toluene	0.5	66
6	Fe ₃ O ₄ -SAHPG ₂ -Pd ⁰	Toluene	1	91
7	Fe ₃ O ₄ -SAHPG ₂ -Pd ⁰	Toluene	2	91
8	Fe ₃ O ₄ -SAHPG ₂ -Pd ⁰	Toluene	5	92
9	Fe ₃ O ₄ -SAHPG ₂ -Pd ⁰	Acetonitrile	1	89
10	Fe ₃ O ₄ -SAHPG ₂ -Pd ⁰	DMF	1	56

Note: Reaction conditions: *N*-methyl-*N*-phenylpyrimidin-4-amine (1 mmol), 1.2 equiv. K₂CO₃, 3-ml solvent, 60°C, 2 h.



SCHEME 6 Scope of the pyrimido[4,5-*b*]indoles

the Supporting Information for more detailed information.

3.3 | General procedure for the synthesis of compounds 5

A Carius tube was charged with compound **4** (1 mmol), $\text{Fe}_3\text{O}_4\text{-SAHPG}_2\text{-Pd}^0$ (1 mol% of Pd loading), K_2CO_3 (1.5 equiv.), and a magnetic stirrer. Dry toluene (3 ml) was added, and the tube was sealed. The reaction mixture was stirred in a preheated oil bath at 60°C for 2 h. After cooling the tube, the crude was diluted with CH_2Cl_2 (20 ml) and filtered through a Celite pad. The filtrate was concentrated, and the crude was purified by column chromatography (silica gel, *n*-hexane/EtOAc, gradient from 0% to 10% EtOAc) to afford pyrimido[4,5-*b*]indoles **5**. See the Supporting Information for more detailed information.

(0.50– ∞). See the Supporting Information for more

(0.59 g). See the Supporting Information for more detailed information.

3.2 | General procedure for the synthesis of biaryl compounds

Fe_3O_4 -SAHPG-Pd⁰ (0.1 mol%, calculated according to the ICP analysis) was added to a solution of aryl halide (1 mmol) and arylboronic acid (1 mmol) in H₂O (3 ml). The resulting suspension was stirred at room temperature for 1 h. After the reaction was completed (monitored by TLC), the catalyst was removed from the crude by external magnet field and washed with water (3 × 2 ml) and chloroform (3 × 5 ml). Then, the organic phase was dried over MgSO₄ and concentrated by rotary evaporation. The resulting crude product was purified by column chromatography over silica gel to obtain the final product. See

4 | CONCLUSION

In summary, we have introduced an eco-friendly and magnetic quasiheterogeneous catalytic system Fe_3O_4 -SAHPG₂-Pd⁰ that is very efficient for the Suzuki-Miyaura cross-coupling reaction of aryl halides with aryl boronic acids at room temperature and in aqueous media. The SAHPG, prepared by ring-opening polymerization in a one-pot process, proved to be an excellent support for the dispersion of Fe_3O_4 NPs in polar solvents, as well as good stabilizer of the Pd NPs via coordination with the terminal hydroxyl groups and ether moieties present in SAHPG. The Fe_3O_4 -SAHPG₂-Pd⁰ catalyst showed high

stability and recyclability, being a ligand-free catalyst with short reaction times especially for aryl chlorides. The easy separation of the catalyst, a negligible leaching, and low loadings of catalyst and use of water as green solvent for Suzuki–Miyaura coupling are significant advantages of this catalyst. Also, we have uncovered a new path to synthesize pyrimido[4,5-*b*]indole via oxidative addition/C–H activation reactions on the pyrimidine ring that can be effectively catalyzed by Fe_3O_4 -SAHPG₂-Pd⁰.

ACKNOWLEDGMENTS

The authors gratefully acknowledge Research Council of Ferdowsi University of Mashhad (Grant 3/41215), MICINN (Grant PGC2018-100719-B-I00 with FEDER funding), and Fundación Séneca Región de Murcia (Grant 19890/GERM/15) for supporting this study. The authors gratefully acknowledge Prof. Isabel María Saura and Prof. María Teresa Chicote for their support during the current work.

AUTHOR CONTRIBUTIONS

Hamid Azizollahi: Conceptualization; data curation; formal analysis; investigation; methodology; validation; visualization. **Hossein Eshghi:** Conceptualization; data curation; formal analysis; funding acquisition; investigation; methodology; project administration; resources; supervision; validation. **José-Antonio García-López:** Data curation; formal analysis; investigation; methodology; validation; visualization.

CONFLICT OF INTEREST

There are no conflicts to declare.

DATA AVAILABILITY STATEMENT

The data that supports the findings of this study are available in the supplementary material of this article.

ORCID

Hamid Azizollahi  <https://orcid.org/0000-0002-3634-2200>

Hossein Eshghi  <https://orcid.org/0000-0002-8417-220X>
José-Antonio García-López  <https://orcid.org/0000-0002-8143-7081>

REFERENCES

- [1] H. Shinokubo, K. Oshima, *Eur. J. Org. Chem.* **2004**, 2004, 2081.
- [2] W. Shi, C. Liu, A. Lei, *Chem. Soc. Rev.* **2011**, 40, 2761.
- [3] M. I. Lipschutz, T. D. Tilley, *Angew. Chem., Int. Ed.* **2014**, 126, 7418.
- [4] M. M. Heravi, Z. Kheirkordi, V. Zadsirjan, M. Heydari, M. Malmir, *J. Organomet. Chem.* **2018**, 861, 17.
- [5] K. C. Nicolaou, P. G. Bulger, D. Sarlah, *Angew. Chem., Int. Ed.* **2005**, 44, 4442.
- [6] A. Fihri, M. Bouhrara, B. Nekoueishahraki, J.-M. Basset, V. Polshettiwar, *Chem. Soc. Rev.* **2011**, 40, 5181.
- [7] A. Bulut, M. Aydemir, F. Durap, M. Gülcen, M. Zahmakiran, *ChemistrySelect* **2018**, 3, 1569.
- [8] M. Nasrollahzadeh, *Molecules* **2018**, 23, 2532.
- [9] B. Dutta, S. Omar, S. Natour, R. Abu-Reziq, *Catal. Commun.* **2015**, 61, 31.
- [10] A. Biffis, M. Zecca, M. Basato, *J. Mol. Catal. A: Chem.* **2001**, 173, 249.
- [11] N. Gogoi, U. Bora, G. Borah, P. K. Gogoi, *Appl. Organomet. Chem.* **2017**, 31, e3686.
- [12] J. Zhi, D. Song, Z. Li, X. Lei, A. Hu, *Chem. Commun.* **2011**, 47, 10707.
- [13] S. J. Tabatabaei Rezaei, H. Khorramabadi, A. Hesami, A. Ramazani, V. Amani, R. Ahmadi, *Ind. Eng. Chem. Res.* **2017**, 56, 12256.
- [14] F. Adibian, A. R. Pourali, B. Maleki, M. Baghayeri, A. Amiri, *Polyhedron* **2020**, 175, 114179.
- [15] F. Diler, H. Burhan, H. Genc, E. Kuyuldar, M. Zengin, K. Cellat, F. Sen, *J. Mol. Liq.* **2019**, 111967.
- [16] M. Seiler, *Fluid Phase Equilib.* **2006**, 241, 155.
- [17] G. Jiang, W. Chen, W. Xia, *Monomers Polym.* **2008**, 11, 105.
- [18] S. J. Tabatabaei Rezaei, A. Shamseddin, A. Ramazani, A. Mashhadi Malekzadeh, P. Azimzadeh Asiabi, *Appl. Organomet. Chem.* **2017**, 31, e3707.
- [19] H. Li, J. K. Jo, L. D. Zhang, C.-S. Ha, H. Suh, I. Kim, *Langmuir* **2010**, 26, 18442.
- [20] C. Deraedt, L. Salmon, L. Etienne, J. Ruiz, D. Astruc, *Chem. Commun.* **2013**, 49, 8169.
- [21] I. Favier, D. Pla, M. Gómez, *Chem. Rev.* **2020**, 120, 1146.
- [22] S. Luo, X. Hu, Y. Zhang, C. Ling, X. Liu, S. Chen, *Polym. J.* **2011**, 43, 41.
- [23] M. Liu, J. M. J. Fréchet, *Pharm. Sci. Technol. To.* **1999**, 2, 393.
- [24] M. Kim, F. M. MacDonnell, M. E. Gimon-Kinsel, T. Du Bois, N. Asgharian, J. C. Griener, *Angew. Chem., Int. Ed.* **2000**, 39, 615.
- [25] R. M. Crooks, M. Zhao, L. Sun, V. Chechik, L. K. Yeung, *Acc. Chem. Res.* **2001**, 34, 181.
- [26] Y. Zhou, D. Yan, *Chem. Commun.* **2009**, 1172.
- [27] H. Jin, W. Huang, X. Zhu, Y. Zhou, D. Yan, *Chem. Soc. Rev.* **2012**, 41, 5986.
- [28] Y. Zhou, W. Huang, J. Liu, X. Zhu, D. Yan, *Adv. Mater.* **2010**, 22, 4567.
- [29] H. Alinezhad, M. Tarahomi, B. Maleki, A. Amiri, *Appl. Organomet. Chem.* **2019**, 33, e4661.
- [30] M. Tarahomi, H. Alinezhad, B. Maleki, *Appl. Organomet. Chem.* **2019**, 33, e5203.
- [31] B. Maleki, E. Sheikh, E. R. Seresht, H. Eshghi, S. S. Ashrafi, A. Khojastehnezhad, H. Veisi, *Org. Prep. Proced. Int.* **2016**, 48, 37.
- [32] B. Maleki, O. Reiser, E. Esmaeilnezhad, H. J. Choi, *Polyhedron* **2019**, 162, 129.
- [33] A. Jamshidi, B. Maleki, F. M. Zonoz, R. Tayebi, *Mater. Chem. Phys.* **2018**, 209, 46.
- [34] C. Deraedt, D. Astruc, *Acc. Chem. Res.* **2014**, 47, 494.
- [35] X. Tang, S. Zhou, X. Tao, J. Wang, F. Wang, Y. Liang, *Mater. Sci. Eng. C* **2017**, 75, 1042.
- [36] L. M. de Espinosa, G. L. Fiore, C. Weder, E. Johan Foster, Y. C. Simon, *Prog. Polym. Sci.* **2015**, 49–50, 60.

- [37] Y. Liu, G. Zhan, X. Zhong, Y. Yu, W. Gan, *Liq. Cryst.* **2011**, *38*, 995.
- [38] C. R. Martinez, B. L. Iverson, *Chem. Sci.* **2012**, *3*, 2191.
- [39] L. Pan, J. Ban, S. Lu, G. Chen, J. Yang, Q. Luo, L. Wu, J. Yu, *RSC Adv.* **2015**, *5*, 60596.
- [40] V. Polshettiwar, R. Luque, A. Fihri, H. Zhu, M. Bouhrara, J.-M. Basset, *Chem. Rev.* **2011**, *111*, 3036.
- [41] B. Liu, W. Zhang, F. Yang, H. Feng, X. Yang, *J. Phys. Chem. C* **2011**, *115*, 15875.
- [42] H. Bai, Z. Liu, D. D. Sun, *Sep. Purif. Technol.* **2011**, *81*, 392.
- [43] W. Song, M. Liu, R. Hu, X. Tan, J. Li, *Chem. Eng. J.* **2014**, *246*, 268.
- [44] A. H. Rezayan, M. Mousavi, S. Kheirjou, G. Amoabediny, M. S. Ardestani, J. Mohammadnejad, *J. Magn. Magn. Mater.* **2016**, *420*, 210.
- [45] Y. Wang, Y. Liu, W. Zhang, H. Sun, K. Zhang, Y. Jian, Q. Gu, G. Zhang, J. Li, Z. Gao, *ChemSusChem* **2019**, *12*, 5265.
- [46] P. R. Boruah, P. S. Gehlot, A. Kumar, D. Sarma, *Mol. Catal.* **2018**, *461*, 54.
- [47] M. H. Salehi, M. Yousefi, M. Hekmati, E. Balali, *Polyhedron* **2019**, *165*, 132.
- [48] W. Xu, C. Liu, D. Xiang, Q. Luo, Y. Shu, H. Lin, Y. Hu, Z. Zhang, Y. Ouyang, *RSC Adv.* **2019**, *9*, 34595.
- [49] P. Akbarzadeh, N. Koukabi, E. Kolvari, *Mol. Diversity* **2019**. <https://doi.org/10.1007/s11030-019-10016-x>
- [50] H. Targhan, A. Hassanpour, K. Bahrami, *Appl. Organomet. Chem.* **2019**, *33*, e5121.
- [51] Y. Han, J.-Q. Di, A.-D. Zhao, Z.-H. Zhang, *Appl. Organomet. Chem.* **2019**, *33*, e5172.
- [52] M. Keyhaniyan, A. Shiri, H. Eshghi, A. Khojastehnezhad, *Chem* **2018**, *42*, 19433.
- [53] P. Dutta, A. Sarkar, *Adv. Synth. Catal.* **2011**, *353*, 2814.
- [54] D. Paul, S. Rudra, P. Rahman, S. Khatua, M. Pradhan, P. N. Chatterjee, *J. Organomet. Chem.* **2018**, *871*, 96.
- [55] K. Inada, N. Miyaura, *Tetrahedron* **2000**, *56*, 8657.
- [56] H. D. H. Showalter, A. J. Bridges, H. Zhou, A. D. Sercel, A. McMichael, D. W. Fry, *J. Med. Chem.* **1999**, *42*, 5464.
- [57] V. P. Borovik, O. P. Shkurko, *Russ. Chem. Bull.* **2002**, *51*, 2129.
- [58] V. V. Lapachev, W. Stadlbauer, T. Kappe, *Monatsh. Chem.* **1988**, *119*, 97.
- [59] Y.-M. Zhang, T. Razler, P. F. Jackson, *Tetrahedron Lett.* **2002**, *43*, 8235.

SUPPORTING INFORMATION

Additional supporting information may be found online in the Supporting Information section at the end of this article.

How to cite this article: Azizollahi H, Eshghi H, García-López J-A. Fe₃O₄-SAHPG-Pd⁰ nanoparticles: A ligand-free and low Pd loading quasiheterogeneous catalyst active for mild Suzuki–Miyaura coupling and C–H activation of pyrimidine cores. *Appl Organomet Chem.* 2020; e6020. <https://doi.org/10.1002/aoc.6020>